

## CALCULATION OF OPTICAL PARAMETERS OF a-Ge-Se-Sn THIN FILMS

A. Thakur, V. Sharma, G. S. S. Saini, N. Goyal, S. K. Tripathi\*

Centre of Advanced Study in Physics, Panjab University, Chandigarh-160 014, India

The present paper reports the effect of Sn impurity on the optical properties of  $\text{Ge}_{20}\text{Se}_{80}$  glassy alloy. Thin films of  $\text{Ge}_{20}\text{Se}_{80}$  and  $(\text{Ge}_{20}\text{Se}_{80})_{90}\text{Sn}_{10}$  alloys have been prepared by thermal evaporation technique. The optical transmission spectra of the substrate with and without of these amorphous thin films have been measured in the spectral range of 400 nm to 2000 nm. Refractive index (n) and thickness (d) of the films have been calculated using an optical characterization method based on creating the upper and lower envelope curves of the spectrum. The value of n increases after the Sn addition. These values of n have been fitted to the single oscillator model. The value of oscillator strength ( $E_d$ ) increases and average energy gap ( $E_0$ ) decreases after the Sn incorporation. The optical absorption edge is described using the non-direct transition model proposed by Tauc and the optical band gap ( $E_g^{\text{opt}}$ ) is calculated from the absorption coefficient ( $\alpha$ ) values by Tauc's extrapolation procedure. The value of  $E_g^{\text{opt}}$  and disorder parameter ( $B^{1/2}$ ) decrease with the Sn addition. The dispersion of the refractive index is explained in terms of the single-oscillator-model. The decrease of the optical gap ( $E_g^{\text{opt}}$ ) has been explained on the basis of difference on the binding energies of different bonds which are arising due to the incorporation of Sn into a- $\text{Ge}_{20}\text{Se}_{80}$  thin films.

(Received July 4, 2005; accepted July 21, 2005)

*Keywords:* Chalcogenide glasses, Optical properties, Band gap

### 1. Introduction

Chalcogenide glasses are very promising materials for use in the guided wave devices and infrared telecommunication systems [1]. High optical transparency in the near and far infrared region as well as large optical non-linearity are two important and attractive optical properties of these materials used in linear and non-linear integrated optical elements. The low characteristic vibrational frequencies of chalcogenide bonds allow them to transmit far out into the infrared [2]. These glasses show a variety of photo-stimulated phenomena when exposed to light or other radiations [3-7]. When these glasses are irradiated with high energy particles or light, bond breaking and bond rearrangement can take place, which results in the change in local structure of the glassy materials. These include subtle effects such as shifts in the absorption edge (photo-bleaching and photo-darkening), and more substantial atomic and molecular reconfiguration such as photo-induced refractive index changes and photo-doping effects [8,9]. In general, these phenomena are associated with the changes in the optical constants [10,11] and absorption edge shift [12], allowing the use of these materials in the fabrication of a large number of optical devices. Therefore, the determination of the optical parameters of chalcogenide glasses is very important, not only in order to know the basic mechanisms underlying these phenomena, but also to exploit and develop their technological applications.

Chalcogenide glasses like Ge-Se are known to be very good covalently bonded glass formers. The dominant feature of the network is fourfold coordinated Ge. The structure of these glasses is a function of composition [13-15]. A discontinuity in various physical properties of these

---

\* Corresponding author: surya@pu.ac.in; surya\_tr@yahoo.com

glasses has been observed at a composition with the average coordination number  $\langle r \rangle = 2.4$  [16]. The coordination number of Ge is 4 and Se is 2, so at  $x = 20$ , the value of  $\langle r \rangle = 2.4$  in a- $\text{Ge}_x\text{Se}_{100-x}$  system. In the Se rich zone, the structure consists of Se chains linked by Ge atoms tetrahedrally coordinated by Se atoms i.e. the structure consists of chains of corner shared  $\text{GeSe}_{4/2}$ . As the Ge concentration increases, the corner shared tetrahedrons give place to edge shared ones [13-15]. It has been reported that at a concentration about 20 at. % of Ge, a new non-crystalline compound  $\text{GeSe}_4$  exists in the Ge-Se system [17]. Boolchand et al [18] have also observed the evidence of two rigidity transitions as monitored by compositional trends in corner-sharing ( $v_{\text{CS}}$ ) and edge-sharing ( $v_{\text{ES}}$ )  $\text{Ge}(\text{Se}_{1/2})$  mode frequencies in  $\text{Ge}_x\text{Se}_{1-x}$  glasses at  $0 < x < 1/3$  by Raman scattering measurements. A second order transitions from a floppy to an unstressed rigid phase occurs near  $x = 0.20$ , where both  $v_{\text{CS}}(x)$  and  $v_{\text{ES}}(x)$  show a kink. What happens to the  $\text{Ge}_{20}\text{Se}_{80}$  system, when it is alloyed with a second element of group IV, is very important from the basic as well as application point of view. Sn belongs to the IV group and its atomic radii (1.41 Å) is more than the Ge (1.22 Å). A lot of studies have been done on Ge-Sn-Se system at higher concentration of Ge ( $\geq 33$ ) [19-22], but not much work has been done at lower concentrations of Ge ( $\leq 30$ ).

Therefore, the authors have decided to study the effect of Sn additive on the optical properties of such a technically important material. In this paper, a relative simple method for determining the optical constants, using only transmission spectra, based upon Swanepoel [23,24] method has been used. This method is based on the upper and lower envelopes of the optical transmission spectra and very useful when the film thickness is non-uniform. Thin films of a- $\text{Ge}_{20}\text{Se}_{80}$  and a- $(\text{Ge}_{20}\text{Se}_{80})_{90}\text{Sn}_{10}$  have been deposited onto Corning 7059 glass substrates by vacuum thermal evaporation technique. Optical transmission spectra has been taken in the wavelength range 400 nm – 2000 nm. The optical parameters like refractive index ( $n$ ), absorption coefficient ( $\alpha$ ), oscillator strength ( $E_d$ ), oscillator energy ( $E_0$ ), optical gap ( $E_g^{\text{opt}}$ ) have been calculated. The experimental details and the characteristics of the samples are described in Section 2. The results have been presented and discussed in section 3. The last section deals with the conclusions of the present work.

## 2. Experimental procedure

Glassy alloys of  $\text{Ge}_{20}\text{Se}_{80}$  and  $(\text{Ge}_{20}\text{Se}_{80})_{90}\text{Sn}_{10}$  are prepared by quenching technique. Materials (99.999% pure) are weighed according to their atomic percentages and sealed in quartz ampoules in a vacuum  $\sim 2 \times 10^{-5}$  mbar. The sealed ampoules are kept inside a furnace where the temperature is increased up to 1000 °C at a heating rate of 2-3 °C/min. The ampoules are frequently rocked for 24 hours at the highest temperature to make the melt homogeneous. The quenching is done in liquid  $\text{N}_2$ . Thin films of the alloys are prepared by vacuum evaporation technique on well-degassed Corning 7059 glass substrates at room temperature and base pressure of  $\sim 2 \times 10^{-5}$  mbar using a Molybdenum boat. Amorphous nature of the samples have been checked by X-ray diffraction technique. No prominent peak has been observed in the thin film of these alloys.

The normal incidence transmission spectra of the substrate with and without a- $\text{Ge}_{20}\text{Se}_{80}$  and a- $(\text{Ge}_{20}\text{Se}_{80})_{90}\text{Sn}_{10}$  thin films have been measured by a double beam UV/VIS/NIR computer controlled spectrometer [Hitachi-330], in the transmission range 400-2000 nm. The spectrometer was set with a suitable slit width of 1 nm in the measured spectral range. All optical measurements have been performed at room temperature (300 K).

## 3. Theory

The model behind Swanepoel's method [23,24] assumes that the sample is a thin film of non-uniform thickness deposited on a transparent substrate having a refractive index 's'. The system is surrounded by the air, whose refractive index is  $n_0 = 1$ . The film has a complex refractive index  $n^* = n - i k$ , where  $n$  is the refractive index and  $k$  the extinction coefficient, which is related to the absorption coefficient,  $\alpha$  through the relation,  $k = \alpha \lambda / 4 \pi$ . The optical constants are obtained by using only the transmission spectrum. According to this method, which is based on the approach of

Manificier et al [25], the refractive index in the region where  $\alpha \approx 0$  is calculated by the following equation:

$$n = \sqrt{N + \sqrt{N^2 - S^2}} \quad (1)$$

where

$$N = 2s \frac{T_{\max} - T_{\min}}{T_{\max} T_{\min}} + \frac{s^2 + 1}{2} \quad (2)$$

where  $s$  is the refractive index of the substrate.  $T_{\max}$  and  $T_{\min}$  are the envelope values at the wavelengths in which the upper and lower envelopes and the experimental transmission spectrum are tangent respectively, as shown in Fig. 1. The values of  $n$  are calculated using equation (1) at wavelengths corresponding to the tangent points.

If  $n_1$  and  $n_2$  are the refractive indices at two adjacent tangent points at  $\lambda_1$  and  $\lambda_2$ , then according to the basic equation for interference fringes

$$2nt = m\lambda \quad (3)$$

where 'm' is an order number. The thickness is given by

$$t = \frac{\lambda_1 \lambda_2}{4(\lambda_1 n_2 - \lambda_2 n_1)} \quad (4)$$

It should be noted that owing to optical absorption, this particular equation is not valid at the interference maxima and minima, but is valid at the tangent points referred to [23]. Using equation (3), new more precise values of the refractive index and the film thickness were determined by a procedure which was explained in detail in [23,24].

The absorption coefficient ( $\alpha$ ) [24] can be calculated from the relation

$$x = \exp(-\alpha t) \quad (5)$$

where  $x$  is absorbance, given by

$$x = \frac{E_M - \sqrt{E_M^2 - (n^2 - 1)^3 (n^2 - s^4)}}{(n - 1)^3 (n - s^2)} \quad (6)$$

and

$$E_M = \frac{8n^2 s}{T_{\max}} + (n^2 - 1)(n^2 - s^2) \quad (7)$$

The absorption coefficient of amorphous semiconductors in the strong-absorption region ( $\alpha \geq 10^4 \text{ cm}^{-1}$ ), assuming parabolic valence and conduction band edges, is given by [26]

$$\alpha(\hbar\omega) = \frac{B(\hbar\omega - E_g^{\text{opt}})^2}{(\hbar\omega)} \quad (8)$$

where  $\hbar\omega$ ,  $E_g^{\text{opt}}$  and  $B$ , represent photon energy, optical gap and an energy independent constant, respectively. Finally, the optical gap is calculated from the intersection of the plot  $(\alpha\hbar\omega)^{1/2}$  vs.  $\hbar\omega$  with the abscissa axis. The refractive index dispersion  $n(\lambda)$  can be fitted by the Wemple-DiDomenico relation [27,28].

Furthermore,  $E_d$  obeys a simple empirical relationship

$$E_d = \beta N_C Z_d N_e \quad (9)$$

where  $\beta$  is constant, which for covalent crystalline and amorphous materials, has a value of 0.4 eV,  $N_c$  is the coordination number of the cation nearest neighbour of the anion,  $Z_a$  is the formal chemical valency of the anion and  $N_e$  is the effective number of the valence electrons per anion.

#### 4. Results and discussion

Fig. 1 shows the optical transmission spectrum of a-Ge<sub>20</sub>Se<sub>80</sub> and a-(Ge<sub>20</sub>Se<sub>80</sub>)<sub>90</sub>Sn<sub>10</sub> thin films.

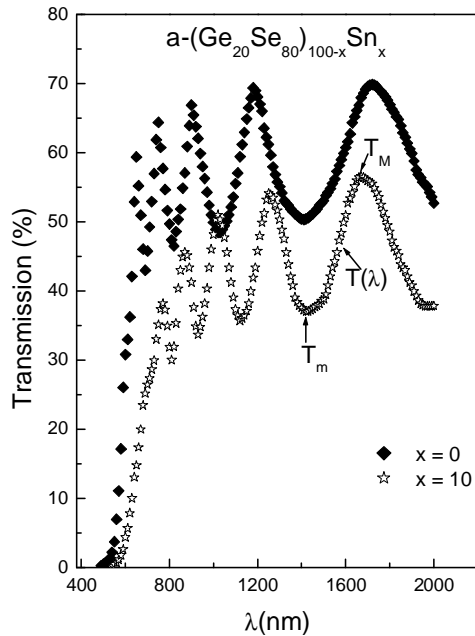


Fig. 1. Transmission spectrum for a-Ge<sub>20</sub>Se<sub>80</sub> and a-(Ge<sub>20</sub>Se<sub>80</sub>)<sub>90</sub>Sn<sub>10</sub> thin films.

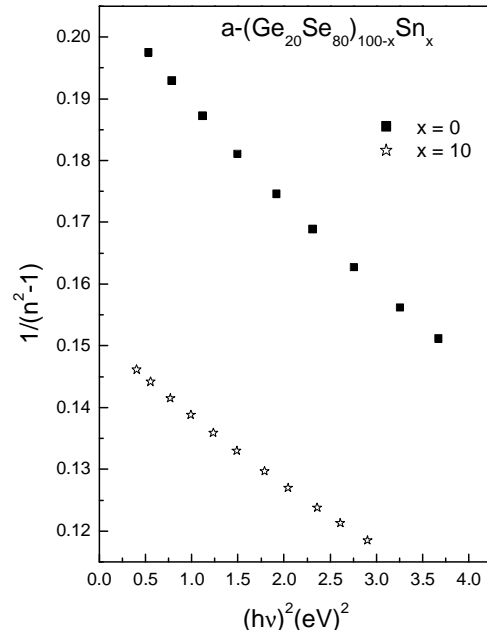


Fig. 2. Plot of  $1/(n^2-1)$  versus  $h\nu$ .

The envelopes of the transmission spectrum,  $T_M$  ( $T_{max}$ ) and  $T_m$  ( $T_{min}$ ) have been observed from this figure. The values of  $n$  are calculated for both samples using equation (1) at different wavelengths corresponding to tangent points ( $T_{max}$  and  $T_{min}$ ) as has been described earlier. On the other hand, the data on the dispersion of the refractive index,  $n(\lambda)$  have been calculated using the single-effective-oscillator model proposed by Wemple and DiDomenico [27,28]. They found that all the data can be described to an excellent approximation by the following relation:

$$n^2(\hbar\omega) = 1 + \frac{E_d E_0}{E_0^2 - (\hbar\omega)^2} \quad (10)$$

where  $\hbar\omega$  is the photon energy,  $E_d$  is oscillator strength and  $E_0$  is the energy of the effective dispersion oscillator (typically near the main peak of the  $\epsilon_2$  - spectrum), which is identified by the mean transition energy from the valence band of the lone-pair state to the conduction-band state (in these amorphous materials, the valence s-states lie far below the top of the valence band, and the valence band involves transitions between lone-pair p-states and antibonding-conduction states [28]). The oscillator energy,  $E_0$ , is an 'average' energy gap, and in close approximation, it scales with the Tauc gap,  $E_g^{opt}$ ,  $E_0 \approx 2 E_g^{opt}$ , as was found by Tanaka [29]. Plotting  $(n^2 - 1)^{-1}$  vs.  $(\hbar\omega)^2$  allows us to determine the oscillator parameters, by fitting a linear function to the smaller energy data. Figure 2 shows the plot of  $(n^2-1)^{-1}$  vs.  $(h\nu)^2$ , which is a straight line.  $E_d$  and  $E_0$  can be directly determined from the slope,  $(E_d E_0)^{-1}$  and the intercept,  $E_0/E_d$ , on the vertical axis. The values of  $E_0$ ,  $E_d$  and static refractive index,  $n(0)$  (i.e. extrapolated to  $\hbar\omega \rightarrow 0$ ) for these alloy thin films are similar to

that of the other Se rich alloys reported in the literature [5,11]. These values are inserted in the Table 1.

The refractive-index dispersion from the Wemple-DeDomenico model is shown in Fig. 3 for both the samples, together with the refractive indexes derived using present characterization method. The value of absorption coefficient ( $\alpha$ ) is calculated at different energy and plotted in Fig. 4. The optical gap ( $E_g^{\text{opt}}$ ) is determined from the intercept on the energy axis of linear fit of the larger energy data, in a plot of  $(\alpha h\nu)^{1/2}$  vs.  $h\nu$  (Tauc extrapolation [26]). Figure 5 shows  $(\alpha h\nu)^{1/2}$  vs.  $h\nu$  for the calculation of  $E_g^{\text{opt}}$ . The values of the refractive index at  $h\omega \rightarrow 0$  [ $n(0)$ ],  $n$ ,  $E_d$ ,  $E_0$ ,  $E_g^{\text{opt}}$ ,  $B^{1/2}$  and cation coordination number ( $N_c$ ) for both the samples are inserted in Table 1.

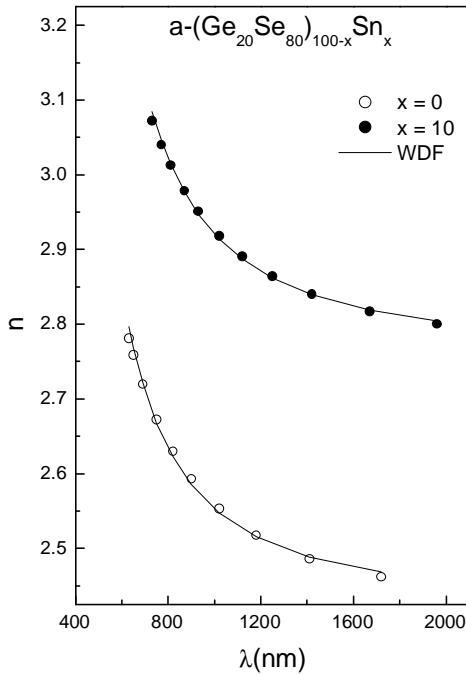


Fig. 3. Variation of experimentally calculated and Wemple -DeDomenico fitted (WDF) values of  $n$  with  $h\nu$ .

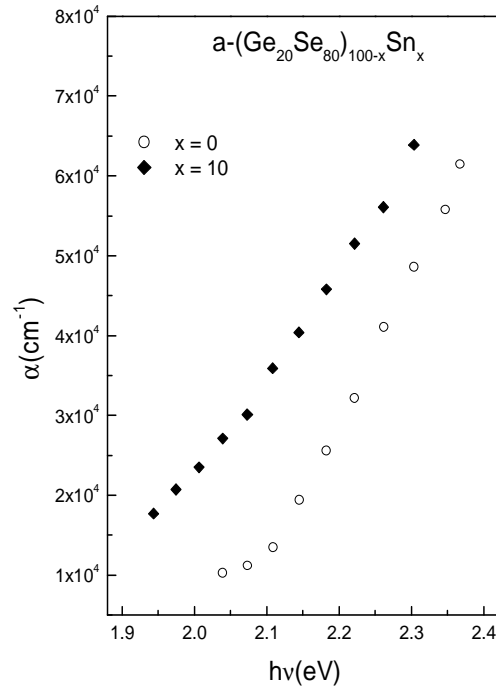


Fig. 4. Variation of  $\alpha$  with  $h\nu$ .

Table 1. Values of the refractive index at  $h\omega \rightarrow 0$  [ $n(0)$ ],  $n$  at 1000 nm, oscillator strength ( $E_d$ ), oscillator energy ( $E_0$ ), Tauc optical gap ( $E_g^{\text{opt}}$ ), disorder parameter ( $B^{1/2}$ ) and cation coordination number ( $N_c$ ).

Composition	$n(0)$	$n$	$E_d$ (eV)	$E_0$ (eV)	$E_g^{\text{opt}}$ (eV)	$B^{1/2}$ ( $\text{cm}^{-1/2} \text{eV}^{-1/2}$ )	$N_c$
$\text{Ge}_{20}\text{Se}_{80}$	2.43	2.56	$18.23 \pm 0.01$	$3.72 \pm 0.01$	$1.94 \pm 0.01$	746	3.26
$(\text{Ge}_{20}\text{Se}_{80})_{90}\text{Sn}_{10}$	2.77	2.92	$24.30 \pm 0.01$	$3.65 \pm 0.01$	$1.68 \pm 0.01$	530	4.02

From these results, it is clear that the values of  $n$  and  $E_d$  are increased and  $E_0$  and  $E_g^{\text{opt}}$  are decreased after the Sn incorporation into the a- $\text{Ge}_{20}\text{Se}_{80}$  glassy alloy. The increase of  $n$  and  $E_d$  can be explained as suggested by Stevens et al. [30]. They have shown the effect of Sn concentration on  $\text{Ge}_{1-x}\text{Sn}_x\text{Se}_2$  glassy system (Ge rich) by indicating several distinct regions. Initially, the Sn concentration does not change the degree of molecular clustering (DMC). In this case, Sn goes preferentially into sites near the raft edges to relieve the strain accumulated there in connection with

the anion homopolar bond states (Se dimers). This process of raft-edge strain relief saturates after some concentration of Sn. But as the concentration of Sn is increased, the role of Sn changes. In this region, DMC increases due to the creation of rafts of smaller lateral extent.

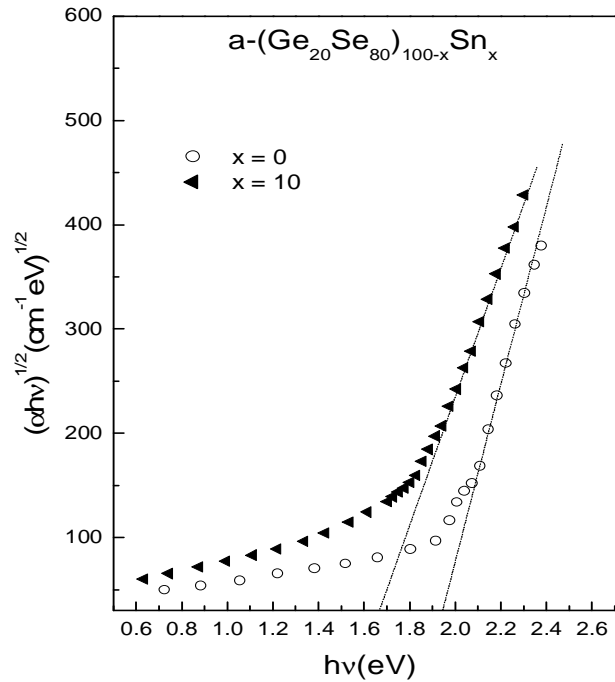


Fig. 5. Plot between  $(\alpha hv)^{1/2}$  and  $hv$ .

Following the above arguments, in our case also, as the concentration of Sn increases, Sn goes preferentially into sites near the raft edges to relieve the strain present due to the anion homopolar bond states (i.e. Se dimers) due to which the value of  $n$  and  $E_d$  increases after the addition of Sn into the binary  $a\text{-Ge}_{20}\text{Se}_{80}$  glassy alloy. Sn will make Sn-Se bonds with the Se present at the raft edges as the binding energy of Sn-Se,  $(401.3 \pm 5.9) \text{ kJ mol}^{-1}$  is much more than the binding energy of Se-Se,  $(162.8 \pm 21) \text{ kJ mol}^{-1}$  due to which the system becomes more rigid. But at higher concentration of Sn, the DMC increases due to the creation of rafts of smaller lateral extent and more ethane-like chains. Evidently, it is energetically more favorably to break up a raft than to introduce strains into its body by replacing smaller Ge atoms (atomic radii,  $1.22 \text{ \AA}$ ) with larger Sn (atomic radii,  $1.41 \text{ \AA}$ ) atoms. The decrease of  $E_g^{\text{opt}}$ , from  $(1.94 \pm 0.01) \text{ eV}$  to  $(1.68 \pm 0.01) \text{ eV}$ , is explained by the fact that the binding energy of the Sn-Se bonds,  $(401.3 \pm 5.9) \text{ kJ mol}^{-1}$ , is smaller than that of the Ge-Se bonds,  $484 \text{ kJ mol}^{-1}$ . Therefore, there is a smaller energy splitting between the states of the valence and conduction bands.

## 6. Conclusions

The optical properties of  $a\text{-Ge}_{20}\text{Se}_{80}$  and  $a\text{-(Ge}_{20}\text{Se}_{80})_{90}\text{Sn}_{10}$  thin films have been measured and calculated from the transmission spectra. The procedure has given refractive indices within a good accuracy. There is a good consistency which has been found between the results obtained in the present work and those previously reported by other authors for related alloys. Incorporation of Sn into the  $a\text{-Ge}_{20}\text{Se}_{80}$  host matrix introduces new Sn-Se chemical bonds, with larger binding energy than that of Se-Se (dimers) and smaller binding energy than that of the Ge-Se bonds, which explains the increase of  $n$ ,  $E_d$  and decrease of the Tauc gap. We have analyzed the optical-dispersion data using the Wemple-DeDomenico single-effective-oscillator model. On the other hand, we

attributed the increase of the oscillator strength,  $E_d$ , with the addition of Sn content. Lastly, the change in the refractive index after the addition of Sn content (10 at %), makes the a-(Ge<sub>20</sub>Se<sub>80</sub>)<sub>90</sub>Sn<sub>10</sub> chalcogenide glass an attractive candidate as optical recording medium.

### Acknowledgements

This work is financially supported by UGC (Major Research Project) New Delhi. AT is grateful to CSIR, New Delhi for providing financial assistance.

### References

- [1] A. V. Stronski, eds. G. Harman, P. Mach, Proceedings of the NATO Advanced Research Workshop on Micro-electronic Interconnections and Assembly, Kluwer Academic, Netherlands, (1998).
- [2] P. J. S. Ewen, C. W. Shinger, A. Zakery, A. Zekak, A. E. Owen, SPIE Infrared Optoelectron. Mater Dev. **1512**, 101 (1991).
- [3] A. Ganjoo, N. Yoshida, K. Shimakawa, Recent Res. Dev. Appl. Phys. **2**, 129 (1999).
- [4] M. S. Iovu, S. D. Shutov, M. Popescu, J. Non-Cryst. Solids **299**, 924 (2002).
- [5] E. Marquez, T. Wagner, J. M. Gonzalez-Leal, A.M. Bernal-Oliva, R. Prieto-Alcon, R. Jimenez-Garay, P. J. S. Ewen, J. Non-Cryst. Solids **274**, 62 (2000).
- [6] A. Arsh, M. Klebanov, V. Lyubin, L. Shapiro, A. Feigel, M. Veinger, B. Sfez, Optical Mat. **26**, 301 (2004).
- [7] V. Lyubin, M. Klebanov, A. Feigel, B. Sfez, J. Non-Cryst. Solids **459**, 183 (2004).
- [8] N. Goyal, A. Zolanvari, S. K. Tripathi, J. Material Science: Materials in Electronics **12**, 523 (2001).
- [9] M. Mitkova, M. N. Kozicki, H. C. Kim, T. L. Alford, J. Non-Cryst. Solids **338**, 552 (2004).
- [10] L. Tichy, H. Ticha, P. Nagels, R. Callaerts, R. Mertens, M. Vlcek, Materials Letters **39**, 122 (1999).
- [11] J. M. Gonzalez-Leal, A. Ledesma, A. M. Bernal-Oliva, R. Prieto-Alcon, E. Marquez, J. A. Angel, J. Carabe, Materials Letters **39**, 232 (1999).
- [12] V. M. Lyubin, M. Klebanov, B. Sfez, B. Ashkinadze, Materials Letters **58**, 1706 (2004).
- [13] X. Feng, W. J. Bresser, P. Boolchand, Phys. Rev. Lett. **78**, 4422 (1997).
- [14] E. Sleafckx, L. Tichy, P. Nagels, R. Callaerts, J. Non-Cryst. Solids **198**, 723 (1996).
- [15] A. Kumar, S. Goel, S. K. Tripathi, Phys. Rev. B **38**, 13432 (1988).
- [16] J. C. Phillips, M. F. Thorpe, Solid State Commun. **53**, 699 (1985).
- [17] A. Feltz, H. Aust, A. Blayer, J. Non-Cryst. Solids **55**, 179 (1983).
- [18] P. Boolchand, X. Feng, W. J. Bresser, J. Non-Cryst. Solids **293**, 348 (2001).
- [19] M. Mitkova, Y. Wang, P. Boolchand, Phys. Rev. Lett. **83**, 3848 (1999).
- [20] Y. Wang, M. Mitkova, D. G. Georgiev, S. Mamedov, P. Boolchand, J. Phys.: Condens. Mat. **15**, S1573 (2003).
- [21] T. Kawaguchi, S. Maruno, S.R. Elliot, J. Appl. Phys. **79**, 9096 (1996).
- [22] H. Tichá, L. Tichý, P. Nagels, E. Sleafckx, R. Callaerts, J. Phys. & Chem. Solids **61**, 545 (2000).
- [23] R. Swanepoel, J. Phys. E: Sci. Instrum. **17**, 896 (1984).
- [24] R. Swanepoel, J. Phys. E **16**, 1214 (1983).
- [25] J. C. Manificier, J. Gasiot, J. P. Fillard, J. Phys. E: Sci. Instrum. **9**, 1002 (1976).
- [26] J. Tauc, J. Non-Cryst. Solids **8**, 569 (1972).
- [27] S. H. Wemple, M. DiDomenico, Phys. Rev. B **3**, 1338 (1971).
- [28] S. H. Wemple, Phys. Rev. B **7**, 3767 (1973).
- [29] K. Tanaka, Thin Solid Films **66**, 271 (1980).
- [30] M. Stevens, J. Grothaus, P. Boolchand, J. G. Hernandez, Sol. St. Commun. **47**, 199 (1983).